

Predicted Exhaust Emissions from a Methanol and Jet Fueled Gas Turbine Combustor

H.G. Adelman,* L.H. Browning,* and R.K. Pefley†
University of Santa Clara, Santa Clara, Calif.

A computer model of a gas turbine combustor has been used to predict the kinetic combustion and pollutant formation processes for methanol and simulated jet fuel. Use of the kinetic reaction mechanisms also has allowed a study of ignition delay and flammability limit of these two fuels. A droplet vaporization scheme has been added to account for the finite vaporization rate and the heat of vaporization of these liquid fuels. The NO_x emissions for methanol were predicted to be from 69 to 92% lower than those for jet fuel at the same equivalence ratio, which is in agreement with experimentally observed results. The high heat of vaporization of methanol lowers both the combustor inlet mixture temperatures and the final combustion temperatures. The lower combustion temperatures lead to low NO_x emissions, whereas the lower inlet mixture temperatures increase methanol's ignition delay. This increase in ignition delay dictates the lean flammability limit of methanol to be $\phi = 0.8$, whereas jet fuel is shown to combust at $\phi = 0.4$. If the amount of recirculation in the combustor primary zone increases with leaner mixtures and lower temperatures, rather than remaining constant as assumed here, then the lean flammability limit of methanol can be extended.

Introduction

IN the future, the pollutants from both mobile and stationary sources will be subjected to more stringent regulation, and the exhaust emissions from jet aircraft and stationary powerplants will have to be reduced to meet these standards. Although progress is being made in the reduction of exhaust emissions from conventionally fueled gas turbines, predicted shortages and the resulting higher costs of hydrocarbon fuels may require the use of alternate fuels. Before suitable alternate fuels can be selected, information on their expected exhaust emissions must be made available.

Methanol now is recognized as an important alternate fuel candidate,¹ which can be produced from coal, vegetation, or timber growth and organic wastes. It can be used to replace conventional fuels in a variety of combustion systems, including gas turbine engines.² The ability of methanol to reduce exhaust emissions while increasing the thermal efficiency of spark ignition piston engines has already been demonstrated.^{3,4}

The properties of methanol which contribute to the reduction of reciprocating engine pollutants, particularly NO_x , are a lower flame temperature and a wider flammability limit than conventional hydrocarbon fuels. This study uses a computer model to predict and compare the emissions from a gas turbine combustor operating on methanol and on jet fuel.

Combustor Model

Primary Zone

Modeling of the primary zone is of major importance since almost all of the pollutants from a gas turbine combustor are formed in this region. Various models for the primary zone of a combustor have been proposed which include plug flow,⁵

stirred reactors,⁶ or combinations of these flow systems in series or in parallel.⁷ Actual flow patterns in the primary zone appear to consist of an embedded recirculation zone surrounded by a flowing stream.⁸ In the recirculation zone, the temperatures are at or near the flame temperature of the combusted air-fuel mixture. The recirculation zone maintains ignition of the air-fuel mixture in the surrounding annular stream tube through a mixing process that provides heat and free radicals. The recirculation mass flow is estimated to be from 10 to 40% of the primary air flow, which is 25% of the total air flow.

The combustor model used here (see Fig. 1), which is patterned after the JT8D, assumes plug flow in the primary zone. In order to simulate the recirculation zone, a fraction of the combusted mixture at the primary zone exit is recirculated and mixed with the incoming air-fuel mixture. This mixing, which is assumed to be adiabatic, complete, and instantaneous, raises the temperature of the inlet mixture and provides the active radicals necessary for short ignition delay. The recirculated gases also contain pollutants, such as unburned fuel, CO, and NO_x . The model therefore accounts for the pollutants arising from both the recirculation zone and from the reacting mixture. A more detailed description of this model appears in Refs. 9 and 10.

In this paper, the total air flow rate through the combustor was held constant at 267.2 moles of air/sec for both fuels at all equivalence ratios. The air flow split between the primary and secondary zone also was held constant at 25%/75% for all conditions. Only the fuel flow rate was varied to provide the changes in equivalence ratios.

Calculation of Recirculation Fraction

As noted earlier, 10 to 40% recirculation has been observed in gas turbine combustors. The amount of recirculation must

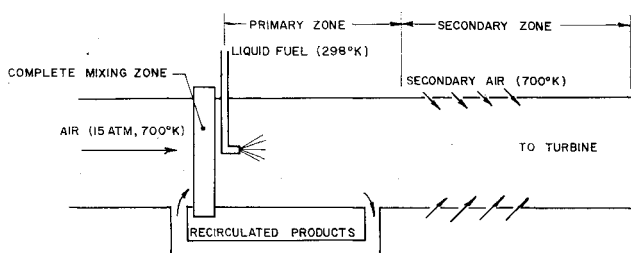


Fig. 1 Combustor model schematic.

Received Sept. 25, 1975; presented as Paper 75-1266 at the AIAA/SAE 11th Propulsion Conference, Anaheim, Calif., Sept. 29-Oct. 1, 1975; revision received Jan. 9, 1975. This work was made possible through a NASA-University support program. The authors wish to thank R.A. Craig for his substantial assistance at the beginning of this project and C. T. Bowman for providing a copy of Ref. 14 prior to publication.

Index categories: Computer Technology and Computer Simulation Techniques; Combustion in Gases; Thermochemistry and Chemical Kinetics.

*Research Associate, Department of Mechanical Engineering.

†Department Chairman, Department of Mechanical Engineering.

Table 1 Methanol oxidation reaction set

Reaction	Forward rate coefficient, k_f^a
1. $\text{CH}_3\text{OH} + \text{M} = \text{CH}_3 + \text{OH} + \text{M}$	$1.0 \times 10^{18} \exp(-34200/T)^b$
2. $\text{CH}_3 + \text{CH}_3\text{OH} = \text{CH}_2\text{OH} + \text{CH}_4$	$1.8 \times 10^{11} \exp(-4940/T)$
3. $\text{O} + \text{CH}_3\text{OH} = \text{CH}_2\text{OH} + \text{OH}$	$1.7 \times 10^{12} \exp(-1150/T)$
4. $\text{H} + \text{CH}_3\text{OH} = \text{CH}_3 + \text{H}_2\text{O}$	$1.3 \times 10^{13} \exp(-2670/T)$
5. $\text{OH} + \text{CH}_3\text{OH} = \text{CH}_2\text{OH} + \text{H}_2\text{O}$	$3.0 \times 10^{14} \exp(-3000/T)^b$
6. $\text{CH}_2\text{OH} + \text{O}_2 = \text{CH}_2\text{O} + \text{HO}_2$	5×10^{10}
7. $\text{CH}_2\text{OH} + \text{M} = \text{CH}_2 + \text{H} + \text{M}$	$2.5 \times 10^{14} \exp(-14600/T)^b$
8. $\text{CH}_4 + \text{OH} = \text{CH}_3 + \text{H}_2\text{O}$	$6 \times 10^{14} \exp(-6290/T)$
9. $\text{CH}_4 + \text{H} = \text{CH}_3 + \text{H}_2$	$2.24 \times 10^4 T^3 \exp(-4400/T)$
10. $\text{CH}_4 + \text{O} = \text{CH}_3 + \text{OH}$	$2.1 \times 10^{13} \exp(-4560/T)$
11. $\text{CH}_3 + \text{O} = \text{CH}_2\text{O} + \text{H}$	1×10^{14}
12. $\text{CH}_3 + \text{O}_2 = \text{CH}_2\text{O} + \text{OH}$	2×10^{10c}
13. $\text{CH}_2\text{O} + \text{OH} = \text{HCO} + \text{H}_2\text{O}$	$5.4 \times 10^{14} (-3170/T)$
14. $\text{CH}_2\text{O} + \text{H} = \text{HCO} + \text{H}_2$	$1.35 \times 10^{13} \exp(-1890/T)$
15. $\text{CH}_2\text{O} + \text{O} = \text{HCO} + \text{OH}$	$5 \times 10^{13} \exp(-2300/T)$
16. $\text{CH}_2\text{O} + \text{M} = \text{HCO} + \text{H} + \text{M}$	$1 \times 10^{14} \exp(-18500/T)$
17. $\text{HCO} + \text{OH} = \text{CO} + \text{H}_2\text{O}$	1×10^{14}
18. $\text{HCO} + \text{H} = \text{CO} + \text{H}_2$	2×10^{14}
19. $\text{HCO} + \text{O} = \text{CO} + \text{OH}$	1×10^{14}
20. $\text{HCO} + \text{M} = \text{CO} + \text{H} + \text{M}$	$5 \times 10^{14} \exp(-9570/T)$
21. $\text{H}_2 + \text{OH} = \text{H}_2\text{O} + \text{H}$	$2.9 \times 10^{14} \exp(-5530/T)$
22. $\text{O} + \text{H}_2 = \text{OH} + \text{H}$	$3.2 \times 10^{14} \exp(-7540/T)$
23. $\text{H} + \text{O}_2 = \text{OH} + \text{O}$	$4.4 \times 10^{14} \exp(-8450/T)$
24. $\text{OH} + \text{OH} = \text{H}_2\text{O} + \text{O}$	$5.5 \times 10^{13} \exp(-3520/T)$
25. $\text{CO} + \text{OH} = \text{CO}_2 + \text{H}$	$4.0 \times 10^{12} \exp(-4030/T)$
26. $\text{H} + \text{HO}_2 = \text{OH} + \text{OH}$	$2.5 \times 10^{14} \exp(-950/T)$
27. $\text{H} + \text{OH} + \text{M} = \text{H}_2\text{O} + \text{M}$	$8.4 \times 10^{21} T^{-2}$
28. $\text{H} + \text{O}_2 + \text{M} = \text{HO}_2 + \text{M}$	$1.5 \times 10^{15} \exp(500/T)$

^aUnits in cm^3 , mole, $^\circ\text{K}$.^bThis study.^cRef. 16.

be sufficient to provide short ignition delays in the stream tube region. Experimental evidence of Mullins¹¹ shows that for an ignition delay of 5 msec, which is the maximum residence time of unburned fuel-air in the JT8D combustor, kerosene vapor must be mixed with vitiated air at a minimum temperature of 1150°K. Since air leaves the compressor at only 700°K, the recirculation must be sufficient to adiabatically raise the final air-fuel-recirculated product mixture temperature to 1150°K. In order to calculate the recirculation fraction, a modified chemical equilibrium program based on Ref. 12 was first used to determine the equilibrium conditions of jet fuel combustion. Jet fuel was simulated by C_8H_{16} as suggested in Ref. 13. In this equilibrium calculation, liquid fuel at 298°K and a stoichiometric quantity of air at 700°K were combusted at 15 atm. A fraction of the combustor products at the resulting adiabatic flame temperature were then mixed with the air and fuel to give a final air-fuel-recirculated product mixture temperature of 1150°K. This recirculation fraction was found to be 32.8%. For the purposes of comparing methanol to jet fuel, the recirculation fraction was held constant for both fuels at all equivalence ratios. There is some experimental evidence⁸ that suggests that the amount of recirculation increases with lower temperatures in a combustor. The effect of more recirculation would be to maintain a high incoming air-fuel mixture temperature and predict leaner flammability limits than those shown for a fixed recirculation fraction.

Secondary Zone

The secondary zone also is modeled as a plug flow reactor in series with the primary zone. Dilution air is added linearly along the secondary zone axis, while mixing is assumed to be complete and instantaneous. The same set of fluid mechanical and kinetic reaction equations are used in the secondary zone as in the primary zone; thus, fuel evaporation, combustion, and pollutant formation continue throughout this zone.

Table 2 Jet fuel oxidation reaction set¹⁷

Reaction	Forward rate coefficient, k_f^a
1. $\text{C}_8\text{H}_{16} + \text{O}_2 = 2\text{C}_4\text{H}_8\text{O}$	$7.5 \times 10^6 T^{1.5} \exp(-7900/T)$
2. $\text{C}_4\text{H}_8\text{O} + \text{O}_2 = \text{HO}_2 + \text{CO} + \text{CH}_3 + \text{C}_2\text{H}_4$	$10^{11} T^{1.5} \exp(-10000/T)$
3. $\text{C}_8\text{H}_{16} + \text{OH} = \text{CH}_2\text{O} + \text{CH}_3 + 3\text{C}_2\text{H}_4$	$6 \times 10^8 T \exp(-4500/T)^b$
4. $\text{CH}_3 + \text{O} = \text{CH}_2\text{O} + \text{H}$	2×10^{13}
5. $\text{CH}_3 + \text{O}_2 = \text{CH}_2\text{O} + \text{OH}$	10^{12}
6. $\text{CH}_2\text{O} + \text{OH} = \text{H}_2\text{O} + \text{CO} + \text{H}$	$10^{14} \exp(-4000/T)$
7. $\text{C}_2\text{H}_4 + \text{O}_2 = 2\text{CH}_2\text{O}$	$3 \times 10^2 T^{2.5}$
8. $\text{C}_2\text{H}_4 + \text{OH} = \text{CH}_3 + \text{CH}_2\text{O}$	$5 \times 10^{13} \exp(-3000/T)$
9. $\text{CH}_2\text{O} + \text{OH} = \text{HCO} + \text{H}_2\text{O}$	$3 \times 10^{14} \exp(-212/T)$
10. $\text{HCO} + \text{M} = \text{CO} + \text{H} + \text{M}$	$2 \times 10^{13} T^{0.5} \exp(-14400/T)$
11. $\text{CH}_3 + \text{H}_2 = \text{CH}_4 + \text{H}$	$6 \times 10^{11} \exp(-5500/T)$
12. $\text{HCO} + \text{OH} = \text{H}_2\text{O} + \text{CO}$	5×10^{13}
13. $\text{C}_2\text{H}_4 = \text{C}_2\text{H}_2 + \text{H}_2$	$7 \times 10^8 \exp(-23250/T)$
14. $\text{C}_2\text{H}_2 + \text{OH} = \text{CH}_3 + \text{CO}$	$10^{13} \times \exp(-3500/T)$
15. $2\text{H} + \text{M} = \text{H}_2 + \text{M}$	$2 \times 10^{18} T^{-1}$
16. $2\text{O} + \text{M} = \text{O}_2 + \text{M}$	$10^{17} T^{-1}$
17. $\text{OH} + \text{H} + \text{M} = \text{H}_2\text{O} + \text{M}$	$7 \times 10^{19} T^{-1}$
18. $\text{H} + \text{O}_2 = \text{OH} + \text{O}$	$2.2 \times 10^{14} \exp(-8400/T)$
19. $\text{O} + \text{H}_2 = \text{OH} + \text{H}$	$1.7 \times 10^{13} \exp(-4730/T)$
20. $\text{H} + \text{H}_2\text{O} = \text{H}_2 + \text{OH}$	$8.4 \times 10^{13} \exp(-10000/T)$
21. $\text{O} + \text{H}_2\text{O} = 2\text{OH}$	$5.7 \times 10^{13} \exp(-9000/T)$
22. $\text{CO} + \text{OH} = \text{CO}_2 + \text{H}$	$5.6 \times 10^{11} \exp(-5400/T)$
23. $\text{HO}_2 + \text{M} = \text{H} + \text{O}_2 + \text{M}$	$2.4 \times 10^{15} \exp(-22950/T)$
24. $\text{HO}_2 + \text{H} = 2\text{OH}$	6×10^{13}

^aUnits in cm^3 , mole, $^\circ\text{K}$.^bThis study.

Methanol Reaction Set

The 28 reactions and rate coefficients describing the combustion of methanol (Table 1) were taken from the shock-tube investigation of Bowman.¹⁴ The rates of several reactions

were changed, as will be explained later. The reactions and their original rates described the combustion of methanol in a highly dilute (94-98% Ar) atmosphere at high temperatures (1545°-2180°K). Although these temperatures are similar to the combustion temperatures in a turbine, a lower temperature range (700°-1300°K) is found in the regions of the combustor where combustion is being initiated. The rates of the combustion reactions during this initiation or induction period determine the ignition delay. In an effort to duplicate turbine combustor conditions, Mullins¹¹ injected many hydrocarbon and alcohol fuels into a heated vitiated air stream at temperatures from 1070°-1300°K and measured the ignition delay, which he defined as the time until a luminous flame appeared.

The experimental conditions used by Mullins were modeled to include the temperature, velocity, and composition of the heated air stream and the injection of liquid methanol. The experimental results of Eisenklam, et al.¹⁵ were used to calculate the vaporization rate of 80- μ droplets of methanol. Available fuel vapor was assumed to mix completely and instantaneously with the air.

To match Mullins' observed ignition delays, it was necessary to increase the rates of reactions 1, 5, and 7 (Table 1) and substitute the rate from Ref. 16 for reaction 12. It should be noted that the lowest temperature for which Mullins determined an ignition delay for methanol was 1152°K. Although the reaction rates have been adjusted to predict the observed delay correctly at 1152°K and 1198°K, they may not predict the correct ignition delay at other temperatures. Such errors would have a significant effect on predicted flammability limits.

Jet Fuel Reaction Set

The set of reactions used to describe the combustion of jet fuel is shown in Table 2, and was taken from Ref. 17. Again, the data from Mullins was used to adjust the rate of reaction 3 to match experimentally observed ignition delays for kerosene vapor at 1140° and 1172°K. Jet fuel has been simulated by C₈H₁₆ as suggested in Ref. 13, since its thermodynamic properties are similar to those of actual jet fuels.

NO_x Reaction Set

The set of reactions describing the formation of NO, NO₂, and N₂O, taken from the literature, is shown in Table 3. In this set of rate equations, the rate of reaction 3 was changed in order to match published experimental emission data for a JT8D engine operating on jet fuel.²⁰ Lowering the rate of this reaction reduced the absolute values of the NO_x emissions for both fuels without changing their relative positions. Hence it is believed that the comparisons made in this paper with the corrected rate predict the correct trends.

Liquid Fuel Vaporization Model

The vaporization of liquid fuel may have a significant effect on the temperatures of the mixture before and after combustion and, therefore, on the ignition delay and the rate of formation of pollutants. Fuel vaporization is particularly important for methanol, which has approximately three times the heat of vaporization of simulated jet fuel. Since roughly twice as much methanol must be used for the same heat input, the net effect is that six times more heat must be absorbed to vaporize methanol. Since the computer simulation was designed to solve gas phase reactions, a scheme was added to

Table 3 NO_x reaction set

Reaction	Forward rate coefficient, k_f^a	Ref.
1. N + NO = N ₂ + O	$3.1 \times 10^{13} \exp(-168/T)$	9
2. N + O ₂ = NO + O	$6.4 \times 10^9 T \exp(-3145/T)$	9
3. N + OH = NO + H	7.0×10^{11}	... ^b
4. H + N ₂ O = N ₂ + OH	$3.0 \times 10^{13} \exp(-5435/T)$	9
5. O + N ₂ O = N ₂ + O ₂	$3.6 \times 10^{13} \exp(-12077/T)$	9
6. O + N ₂ O = NO + NO	$5.0 \times 10^{13} \exp(-12077/T)$	9
7. N + O = NO + M	$6.4 \times 10^{16} T^{-.5}$	9
8. M + N ₂ O = N ₂ + O	$2.0 \times 10^{15} \exp(-29006/T)$	9
9. NO + HO ₂ = NO ₂ + OH	1.0×10^{13}	18
10. NO ₂ + H = NO + OH	$7.2 \times 10^{14} \exp(-971/T)$	18
11. O + NO ₂ = NO + O ₂	$1.9 \times 10^{13} \exp(-533/T)$	18
12. NO ₂ + CO = NO + CO ₂	$1.9 \times 10^{12} \exp(-14724/T)$	19
13. N + N = N ₂ + M	7.0×10^{14}	9
14. H ₂ + NO ₂ = NO + H ₂ O	$2 \times 10^9 \exp(-9058/T)$	18

^aUnits in cm³, mole, K.

^bThis study.

simulate liquid fuel vaporization which assumes an Arrhenius-type equation for liquid fuel vaporization

$$k_v \text{ fuel}(\ell) \rightarrow \text{fuel}(g)$$

where

$$k_v = Ae^{-\Delta E/RT}$$

The values of A and ΔE for methanol were adjusted to simulate the vaporization of fuel droplets in the presence of diffusive burning, using the method of Kollrack and Aceto.¹⁷

Methanol droplets of 150 μ were assumed to be injected at 100 fps relative to the air. This resulted in a value of

$$k_v = 4.6 \times 10^6 e^{-10000/T}$$

The vaporization rate of jet fuel was given in Ref. 17 as

$$k_v = 2 \times 10^5 e^{-5000/T}$$

The effects of fuel vaporization were substantial for methanol in the lean region. As the air-fuel-recirculated product mixture moved along the combustor, the temperature would drop until the fuel began to combust. This temperature drop severely limited the lean flammability limit of methanol. For equivalence ratios leaner than $\phi = 0.8$, the air-fuel mixture was cooled below the temperature that would give ignition of methanol in the combustor. The vaporization of jet fuel did not lower the combustor inlet mixture temperature significantly. Thus, jet fuel showed a much leaner flammability limit of $\phi = 0.4$.

The predicted effects of fuel vaporization suggest that more care must be given to fuel preparation for methanol. If the fuel vaporizes too quickly, inlet mixture temperatures will drop below those necessary for ignition. If very lean methanol mixtures are to be used to reduce pollutants, it may be necessary to pre-vaporize and preheat the fuel.

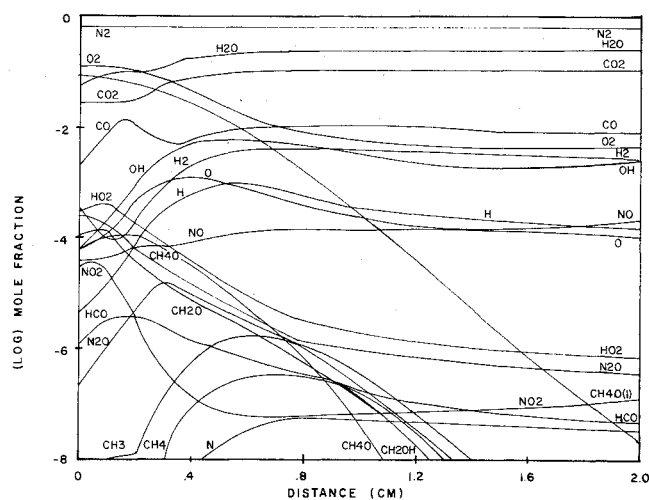
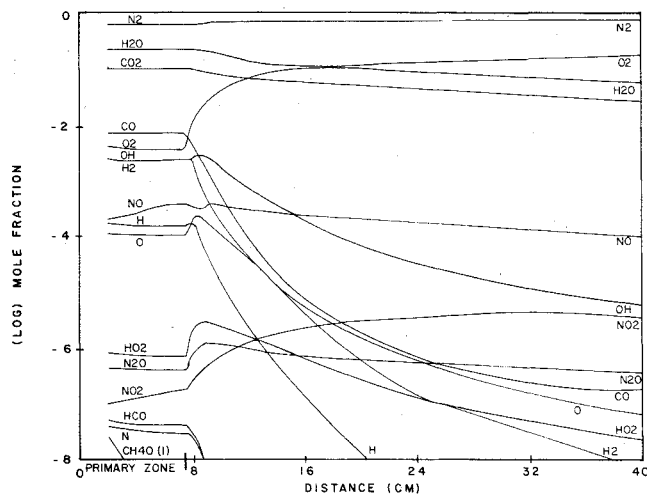
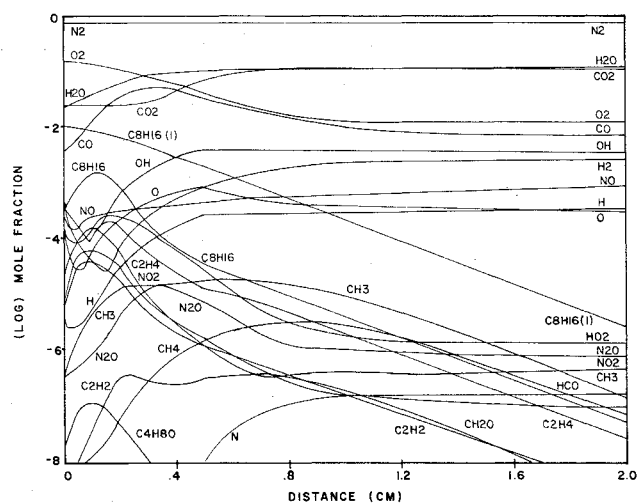
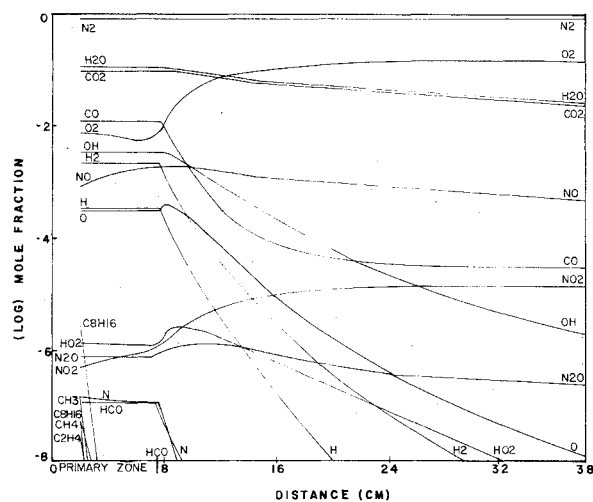
Results

The output of the computer simulation includes histories of temperature and species concentrations in the combustor. Figures 2 and 3 show details of the induction period and the reactions occurring in the flame front for methanol and jet fuel at $\phi = 1.0$. Figures 4 and 5 show species concentrations along the remainder of the primary zone and the secondary zone. The length of the primary zone is 7.62 cm. The species concentrations shown in these figures are typical of the simulations at other values of ϕ .

NO_x Emissions

The emissions of NO_x are shown in Table 4 for both methanol and jet fuel. In order to calculate the amount of

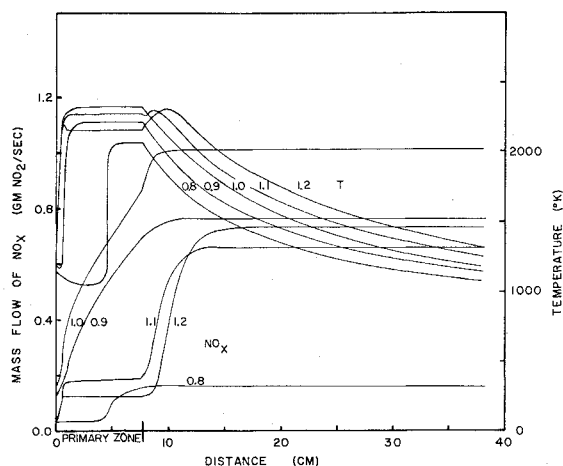
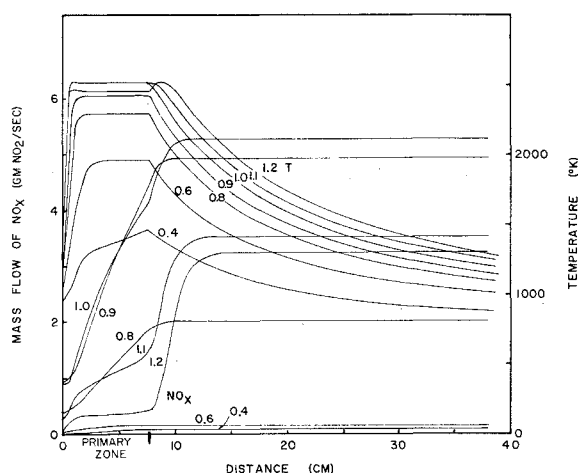
‡A personal communication with James Elwood of Pratt and Whitney Aircraft indicates that the data presented in Ref. 20 are not diluted with the fan bypass air, but represents the actual combustor emissions.

Fig. 2 Combustion details, methanol, $\phi = 1$.Fig. 4 Combustor species, methanol, $\phi = 1$.Fig. 3 Combustion details, jet fuel, $\phi = 1$.Fig. 5 Combustor species, jet fuel, $\phi = 1$.Table 4 Ignition delay, primary zone residence time and NO_x emissions for methanol and jet fuel

ϕ	Ignition delay, msec	Primary zone residence time, msec	Primary zone exit - NO_x not recirculated, NO_x ppm	Primary zone exit - NO_x recirculated, NO_x ppm	Secondary zone exit - NO_x recirculated, NO_x
Methanol					
0.8	3.10	4.22	45	57	15
0.9	0.39	2.79	226	276	73
1.0	0.15	2.60	301	353	108
1.1	0.10	2.56	62	75	65
1.2	0.69	2.55	39	48	72
Jet fuel					
0.4	0.79	4.00	27	30	8
0.6	0.40	3.20	54	66	12
0.8	0.26	2.90	674	815	187
0.9	0.19	2.78	1738	1994	477
1.0	0.16	2.71	1714	1890	525
1.1	0.13	2.67	562	621	353
1.2	0.13	2.65	154	178	324

NO_x in the recirculated gases, the primary zone simulation was first run without recirculated NO_x . The NO_x values at the end of the primary zone (see the first NO_x column, Table 4) then were used to calculate the concentrations of NO_x in the recirculated gases.

For the same equivalence ratio, methanol shows significantly lower NO_x concentrations than jet fuel throughout the combustor. This is related to the fact that methanol has an adiabatic flame temperature that is about 200°K lower than that of jet fuel (see Figs. 6 and 7). Since it is estimated that,

Fig. 6 Temperature and NO_x mass flow rate, methanol.Fig. 7 Temperature and NO_x mass flow rate, jet fuel.

for each 100°K reduction in combustion temperature there is a three-fold reduction in NO_x emissions, it is seen easily why methanol has substantially lower NO_x emissions.

It is interesting to note that for $\phi = 1.20$ the final NO_x level for methanol is slightly higher than for $\phi = 1.10$, even though the concentration is lower in the primary zone. The excess fuel in the case of $\phi = 1.20$ reacts with secondary zone air and continues the formation of NO .

Although most of the NO_x from methanol is predicted to be NO , a few ppm of NO_2 also are predicted. Jet fuel shows higher levels of NO_2 than methanol, with emissions ranging from a low of 1.9 ppm at $\phi = 0.4$ to 11.8 ppm at $\phi = 1.0$. This level of NO_2 is consistent with experimentally observed values of NO_2 from a JT8D combustor, which averaged 12 ppm at full load, whereas NO averaged 226 ppm.²⁰ The NO_2 emissions from methanol ranged from 1.3 ppm at $\phi = 0.8$ to 3.4 ppm at $\phi = 1.0$. Emissions of N_2O were below 1 ppm for all cases, except for jet fuel at $\phi = 0.4$, where they were 6.3 ppm.

Table 4 also shows the ignition delay and primary zone residence times. Previously, NO_x has been assumed to form entirely in the postflame gases with the free radicals O , OH , and H taken at their equilibrium values. The kinetic model used here, however, shows NO formation beginning in the flame front, with the overshoot of O , H , and OH from equilibrium values. In most cases, this value of flame-front NO is insignificant as compared to the postflame concentrations, but in the case of methanol at $\phi = 0.8$, 25 ppm NO appeared in the 0.2 msec following ignition, whereas the remaining 20 ppm was formed during the next 0.9 msec in the postflame gases.

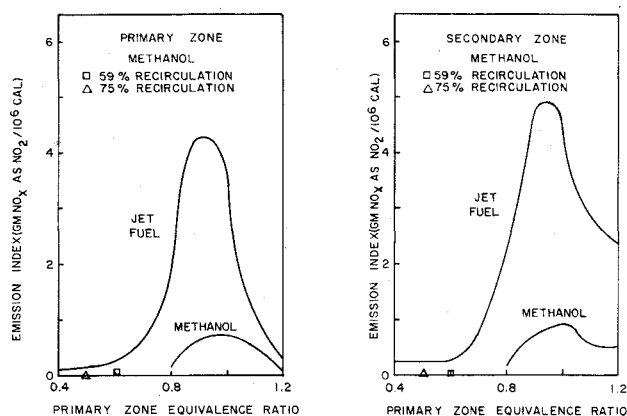
Fig. 8 NO_x emission indices for methanol and jet fuel.

Table 5 CO emissions ppm

ϕ	Primary zone exit		Secondary zone exit	
	Methanol	Jet Fuel	Methanol	Jet fuel
0.4	...	1.67×10^4	...	2123
0.6	...	1145	...	8.1
0.8	246	1433	0.11	18.5
0.9	1143	4707	0.13	22.2
1.0	6338	1.4×10^4 (1.4×10^4)	0.16	24.6
1.1	3.0×10^4	3.3×10^4	0.20	26.1
1.2	5.4×10^4	5.7×10^4	0.26	28.0

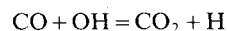
^aBeyond flammability limit.

Table 4 shows the molar concentrations of NO_x , but the mass emissions are shown in Figs. 6 and 7. When comparing emissions from different fuels, it is more appropriate to use an emission index (EI) based on energy input than fuel mass. Consequently, the EI is given in grams of NO_x as NO_2 per million calories, based on the lower heating values of 4764 and 10563 cal/g for methanol and jet fuel, respectively. The NO_x emissions index is substantially lower for methanol than for jet fuel at all equivalence ratios, in both the primary and secondary zones (see Fig. 8). At $\phi = 1.0$, methanol emits only 20% of the NO_x from jet fuel, whereas at $\phi = 0.8$ the level is only 7.7%. Two additional points also are included for methanol at higher recirculation values, which would permit these lean flammability limits. Figures 6 and 7 show that the exit temperatures for methanol are no more than 2% lower than those for jet fuel. Thrust or power levels are dependent upon the product of the exit temperatures and the mass flow rates. Since the total mass flow rates (fuel and air) are found to be 1 to 1.5% higher for methanol, the power levels are virtually identical for both fuels at the same equivalence ratio.

CO Emissions

The CO emissions for methanol and jet fuel are shown in Table 5. In all instances, methanol shows lower CO emissions than jet fuel at the same equivalence ratio. At $\phi = 0.4$ for jet fuel, the low temperatures in the primary zone lead to a sharp increase in CO emissions, which persist through the secondary zone and create the highest level of CO at the combustor exit. Aside from the case of jet fuel at $\phi = 0.4$, CO emissions from the secondary zone are low for both methanol and jet fuel. The predicted CO emissions for jet fuel agree well with experimental data, which show an average of 18 ppm CO emissions from a JT8D engine at 100% load.²⁰ However, other experimental evidence indicates that methanol CO emissions may be three times higher than those for jet fuel.²

An examination of Tables 1 and 2 shows that the rates for the CO oxidation reaction



are different for the two fuel reaction sets, with the rate in the methanol set being 18 times faster at 1500°K than that in the jet fuel set. Since the reaction sets were assumed to be complete and consistent, only the reaction rates that affected ignition delays were changed. However, in order to obtain a direct comparison of CO emissions, the rate for CO oxidation in the methanol set was used to rerun the case of jet fuel at $\phi = 1.0$. CO emissions were identical in the primary zone, whereas the emissions from the secondary zone were decreased by a factor of 100. These new values appear in parentheses in Table 5. With the same CO oxidation rate, the model still predicts lower CO emissions for methanol.

Conclusions

The computer simulation of a gas turbine combustor has predicted levels and trends of NO_x emissions for methanol and jet fuel which are in good agreement with experimentally observed results. The NO_x emissions from methanol are substantially less than for jet fuel at all equivalence ratios where direct comparisons can be drawn. Fuel vaporization significantly affects the ignition delay and NO_x levels of methanol by lowering the temperature of the methanol-air mixtures before and after combustion. Although some experimental data on ignition delay are available for adjusting fuel reaction rates, more data will be required at lower temperatures before conclusions concerning the flammability limits of either methanol or jet fuel can be drawn. A comparison of CO levels was hampered by different CO oxidation rates for the two fuels. However, in one case, where identical CO rates were used, methanol showed slightly lower CO levels than jet fuel, which is opposite to the limited experimental data that are available.

References

- ¹ *Methanol as an Alternate Fuel*, Engineering Foundation Conference, Reprint of Papers, Vol. II, New England College, Henniker, N. H., July 1974.
- ² Jarvis, P. M., "Methanol as Gas Turbine Fuel," presented at the Engineering Foundation Conference, Methanol as an Alternate Fuel, Henniker, N. H., July 1974.
- ³ Adelman, H. G., Andrews, D. G., and Devoto, R. S., "Exhaust Emissions from a Methanol Fueled Automobile," *Society of Automotive Engineers, Transactions*, Vol. 81, 1972.
- ⁴ Pefley, R. K., Saad, M. A., Sweeney, M. A., and Kilgroe, J. D., "Performance and Emission Characteristics Using Blends of Methanol and Dissociated Methanol as an Automotive Fuel," Paper 719008, *Intersociety Energy Conversion Engineering Conference*, Society of Automotive Engineers, Inc., New York, 1971.
- ⁵ Heywood, J. B., Fay, J. A., and Linden, L. H., "Jet Aircraft Air Pollutant Production and Dispersion," *AIAA Journal*, Vol. 9, May 1974, pp. 841-850.
- ⁶ Fletcher, R. S. and Heywood, J. B., "A Model for Nitric Oxide Emissions from Aircraft Gas Turbine Engines," AIAA Paper 71-123, presented at the 9th Aerospace Sciences Meeting, New York, Jan. 1971.
- ⁷ Pratt, D. T., Bowman, B. R., Crowe, C. T., and Sonnichsen, T. C., "Prediction of Nitric Oxide Formation in Turbojet Engines by PSR Analysis," AIAA Paper 71-713, presented at the 7th Propulsion Joint Specialist Conference, Salt Lake City, Utah, 1971.
- ⁸ Rosenthal, J., "Exploratory Methods for the Determination of Gas Flow and Temperature Patterns in Gas Turbine Combustors," Aeronautical Research Laboratories, Department of Supply, Australia, Mech. Eng. Note 235, 1959.
- ⁹ Craig, R. A. and Pritchard, H. O., "Nitric Oxide Production in the presence of Flowing and Combusting H_2 -Air Mixtures," presented at the 1972 Spring Technical Meeting of the Central States Section of the Combustion Institute, Bartlesville, March 1972.
- ¹⁰ Craig, R. A. and Pritchard, H. O., "NO Production in the Secondary Zone of a Turbojet Combustor," presented at the Central States Section of the Combustion Institute, Madison, March 1974.
- ¹¹ Mullins, B. P., "Studies on the Spontaneous Ignition of Fuels Injected into a Hot Air Stream," National Gas Turbine Establishment, England, Repts. 89, 90, 97, and 107, 1952; also *Fuel*, Vol. 32, 1953, p. 343.
- ¹² Gordon, S. and McBride, B. J., "Computer Program for Calculation of Complex Equilibrium Composition, Rocket Performance, Incident and Reflected Shocks and Chapman-Jouguet Detonations," NASA SP-273, 1971.
- ¹³ Roberts, R., Aceto, L. D., Kollrack, R., Bonnell, J. M., and Teixeira, D. P., "An Analytical Model for Nitric Oxide Formation in a Gas Turbine Combustion Chamber," AIAA Paper 71-715, presented at the 7th Propulsion Joint Specialist Conference, Salt Lake City, Utah, 1971.
- ¹⁴ Bowman, C. T., "A Shock-Tube Investigation of the High-Temperature Oxidation of Methanol," to be published.
- ¹⁵ Eisenklam, P., Arunachalam, S. A., and Weston, J. A., "Evaporation Rates and Drag Resistance of Burning Drops," *11th Symposium on Combustion*, The Combustion Institute, 1967, pp. 715-728.
- ¹⁶ Bowman, C. T., "Non-Equilibrium Radical Concentrations in Shock-Initiated Methane Oxidation," *15th Symposium on Combustion*, The Combustion Institute, 1974.
- ¹⁷ Kollrack, R. and Aceto, L. D., "The Effects of Liquid Water Addition in Gas Turbine Combustors," *Journal of APCA*, Vol. 23, Feb. 1973, pp. 116-121.
- ¹⁸ Trotman-Dickenson, A. F. and Milne, G. S., "Tables of Bimolecular Gas Reactions," National Bureau of Standards, Rept., NSRDS-NBS 9, 1967.
- ¹⁹ Kondratiev, V. N., "Rate Constants of Gas Phase Reactions," National Bureau of Standards, Rept., COM-72-10014, 1972.
- ²⁰ Bogdon, L. and McAdams, H. T., "Analysis of Aircraft Exhaust Emission Measurements," Cornell Aeronautical Laboratory, Rept. NA-5007-K-1, Oct. 1971, pp. IV. 222-227.